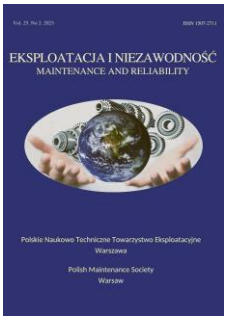

Eksploatacja i Niezawodnosc – Maintenance and Reliability
Volume 28 (2026), Issue 3
journal homepage: http://www.ein.org.pl

Article citation info:
Zhao J, Liang Q, Ye Z, An intelligent key nodes identification method in transportation networks based on gated attention multi-channel GCN, Eksploatacja i Niezawodnosc – Maintenance and Reliability 2026: 28(3) http://doi.org/10.17531/ein/218119

An intelligent key nodes identification method in transportation networks based on gated attention multi-channel GCN

Indexed by: Web of Science Group

Jiangbin Zhao[a,c], Qiyi Liang[a,c], Zhenggeng Ye[b,*]

[a] Department of Intelligence Manufacturing Engineering, Xi'an University of Science and Technology, China
[b] Department of Industrial Engineering, Zhengzhou University, China
[c] Shaanxi Key Laboratory of Mine Electromechanical Equipment Intelligent Detection and Control, Xi'an 710054, China

Highlights

- KeyGAM-GCN integrates structure and attribute features for identifying key nodes.
- SIRS model can generate nodes' labels by considering dynamic spreading influence.
- Gated attention and residual connections can enhance the performance of KeyGAM-GCN.
- ISE and NDCG are used to evaluate propagation efficiency and ranking quality of nodes.

Abstract

The key nodes in Transportation systems can improve the transportation system's performance efficiently and quickly when the maintenance resources are limited. A gated attention multi-channel graph convolutional network (KeyGAM-GCN) is proposed to identify the key nodes for complex transportation networks, which is an intelligent data-driven unsupervised key nodes identification method. In KeyGAM-GCN, a multi-channel graph convolutional network is developed to extract diverse topological and attribute features from transportation networks. A gated attention mechanism can fuse features by adaptively balancing the importance of different feature channels. To validate the effectiveness, experiments on 10 real-world transportation datasets are performed by comparing KeyGAM-GCN with several baselines in multiple metrics. The susceptible-infected-recovered-susceptible model is used to generate the nodes lables for evaluating the performance of the proposed method. The results show that KeyGAM-GCN can provide guidance for preventive maintenance for transportation systems.

Keywords
key node identification, gated attention, transportation networks, SIRS model.

1. Introduction

Transportation networks constitute key infrastructure for modern urban functioning, facilitating essential urban mobility, logistics operations, and emergency response systems [1]. The rapid pace of urbanization coupled with surging transportation demands has led to unprecedented expansion and increasing complexity in transport networks, critically straining their capacity to ensure operational stability, service efficiency, and systemic resilience [2]. Identifying critical nodes, such as major transportation hubs, key intersections, and strategic ports, within these intricate systems is vital for traffic flow optimization, resilience enhancement, and transportation maintenance under limited resources [3]. When natural disasters or major accidents occur, failure of these critical nodes can trigger system-wide paralysis, causing substantial economic damage and societal disruption. Key node identification also intersects with other crucial research domains, including congestion analysis [4], network robustness assessment [5], and cascading failure modeling [6]. Therefore, a sophisticated

(*) Corresponding author.
E-mail addresses: J. Zhao (ORCID: 0000-0002-3034-6710), zhaojiangbin@xust.edu.cn, Q. Liang (ORCID: 0009-0002-3211-3109) liangqiyi@stu.xust.edu.cn, Z. Ye (ORCID: 0000-0002-0636-9701) yezhenggeng@zzu.edu.cn

method for identifying key nodes enables targeted traffic control strategies, optimal resource distribution, and development of highly resilient transportation infrastructure, ultimately safeguarding urban networks' continuous operation and stability.

Complex network theory offers a robust analytical framework for understanding complex systems, revealing their structural properties and operational dynamics [7]. Indeed, many real-world systems are modeled as complex networks, encompassing transportation systems [8], social systems [9], biological systems [10], power systems [11], and citation networks. These networks are characterized by numerous nodes and edges, wherein key nodes significantly impact the holistic structure and functionality. Identifying these key nodes is crucial for a deeper understanding of network topology; it reveals critical aspects of inter-node connectivity and information transmission pathways, thereby illuminating the mechanisms that govern network operations. Accordingly, key node identification constitutes a fundamental problem in complex network research, having garnered widespread interdisciplinary interest in recent years.

Numerous algorithms have been proposed to address key node identification, including classical centrality measures such as Degree Centrality [12], Betweenness Centrality [13], Closeness Centrality [14], k-shell decomposition [15], Eigenvector Centrality [16], H-index [17], and Katz Centrality [18]. These classical centrality-based indicators primarily assess the structural importance of nodes by quantifying their topological significance within a network. Although such methods furnish valuable perspectives on network architecture, they are individually encumbered by inherent constraints. Consequently, relying exclusively on any single metric may prove insufficient for accurately identifying key nodes in complex systems like transportation networks, thereby restricting their practical applicability in real-world scenarios.

Recently, deep learning methods have demonstrated remarkable progress in key node identification tasks and are increasingly utilized in transportation network analysis. In contrast to conventional centrality indicators, deep learning models autonomously learn high-dimensional features, diminishing the need for manual feature engineering and elevating the precision of key node identification. Specifically, graph neural networks (GNNs) leverage both topological structure and node attributes to refine key node identification within complex networks. For instance, Graph Convolutional Networks (GCNs) aggregate features from neighboring nodes, enabling their embeddings to capture global topological information. Graph Attention Networks [19] employ adaptive attention mechanisms to dynamically assign varying importance to neighboring nodes, which improves the flexibility of information exchange. Graph Sampling-based methods, such as GraphSAGE [20], sample a fixed number of neighbors to mitigate computational overhead in large-scale graphs, thereby enhancing model scalability. Moreover, graph cascade learning methods, including InfGCN [21] and DiffPool [22], incorporate information propagation dynamics to model node influence, thus bolstering the robustness of key node identification. Nevertheless, existing approaches still have some limitations, such as insufficient fusion of heterogeneous data and a lack of adaptive mechanisms for feature integration, which curtails their effectiveness in complex transportation networks.

To overcome these challenges, this paper proposes a Gated Attention Multi-Channel Graph Convolutional Network (KeyGAM-GCN), a novel approach for identifying key nodes in transportation networks. The KeyGAM-GCN model operates on two core principles as follows. (1) A multi-channel graph convolutional structure is utilized to holistically capture topological features, traffic flow patterns, and their interactions, enabling effective feature integration. (2) A gated attention mechanism is introduced to dynamically learn the significance of different channels, facilitating adaptive feature fusion and thereby improving both the precision and generalizability of key node identification. The main contributions of the research work are as follows.

- Leveraging the SIRS model to generate the importance labels of nodes, thereby reframing key node identification as a binary classification task. This allows the model to capture node influence within network propagation dynamics, leading to improved identification accuracy. Compared to traditional methods, this approach offers a more accurate reflection of nodal roles in dynamic spreading processes.
- Designing a gated attention mechanism to adaptively fuse multi-channel feature information, enhancing the

model's adaptability to different scenarios. The GAM mechanism automatically adjusts the importance of each feature channel based on data distribution, improving the model's generalization capability.

- Enhancing information interaction via dense residual connections, which strengthens cross-layer feature exchange and mitigates the over-smoothing problem in GNNs. This design preserves key high-level feature information, improving the discriminatory of key nodes.

The remainder of this paper is organized as follows. Section 2 provides a concise review of related work. Section 3 details the proposed KeyGAM-GCN model and the metrics used for its evaluation. Section 4 describes the experimental design, including the datasets, ablation studies, baseline methods, and experimental parameter settings, before presenting an analysis of the experimental outcomes. Section 5 investigates the KeyGAM-GCN model's performance and parameter sensitivity through a case study on the Beijing subway network. Finally, Section 6 summarizes the findings of this study and discusses potential directions for future research.

2. Related work

In recent years, research on key node identification has achieved substantial advancements and found extensive application across diverse domains. In complex network analysis, “centrality” is the generally accepted term for node importance, and this concept has become a focal point, addressing the fundamental question of identifying a network's most pivotal or central vertices. The diverse interpretations of “importance” have culminated in a variety of centrality measures in network analysis [23]. Currently, key node identification methods fall into two main classes: those based on topology and those driven by deep learning. Topology-based methods, including degree centrality, betweenness centrality, and clustering coefficient, ascertain node importance by analyzing network structural features. Deep learning-based methods, typified by Graph Neural Networks (GNNs) like Graph Convolutional Networks (GCNs) and Graph Attention Networks (GATs), identify key nodes through learned representations of features and structure. Both paradigms have substantially contributed to advancing key node identification research.

2.1. Topology-based methods

In complex network analysis, traditional topology-based methods remain fundamental for key node identification. These approaches primarily leverage network topology and assess node importance through various centrality metrics or network features. Based on their analytical perspective, topology-based methods are broadly categorized into local feature-based, global feature-based, and dynamic process-based approaches. Local feature-based methods typically quantify node importance using metrics like degree centrality, betweenness centrality, and closeness centrality. Global feature-based methods, in contrast, consider the overall network structure, employing techniques such as K-shell decomposition and spectral clustering for key node identification. Additionally, dynamic process-based methods have garnered increasing attention. These include approaches grounded in information diffusion models [24], gravity models [25], and random walks [26], which can more accurately capture a node's actual influence by considering its role in dynamic network processes. Within complex transportation network studies, alongside classical centrality measures, several novel metrics have emerged to identify key nodes from diverse perspectives, thereby enhancing identification effectiveness in these systems.

For instance, Wan et al. [27] integrated network centrality with economic factors, proposing a TOPSIS-based comprehensive evaluation method to identify key ports in maritime shipping networks. Wen et al. [28] incorporated joint entropy and multi-scale factors, considering both network topology and port importance to offer a new perspective on transportation network reliability. Bai et al. [29] applied small-group percolation to identify overlapping community structures and key nodes, assessing the resilience and recovery capacity of the global liner shipping network. Xu et al. [30] introduced the motif centrality to identify key ports and optimize the structural robustness of the global liner shipping network.

Furthermore, research has focused on integrating multi-dimensional topological information. Dui et al. [31] combined the Copeland method to rank ports and shipping routes, evaluating the residual resilience of maritime transportation systems. He et al. [32] proposed a modeling and robustness assessment method for multi-modal freight networks, analyzing infrastructure disruption impacts by integrating node and link

characteristics. Du et al. [33] enhanced the topological potential model by incorporating multiple centrality metrics and topological entropy to identify key nodes affecting both structure and passenger flow in metro networks. Sui et al. [34] developed a ship node importance evaluation method based on maritime traffic complex networks to improve waterborne transport safety and efficiency. Curado et al. [35] adopted a multi-layer network centrality approach, constructing a three-layer composite network of urban public transport, commercial activities, and tourism to identify critical areas.

Community structure and network resilience analysis also offer novel perspectives for key node identification [36]. Wandelt et al. [37] utilized the community structure to propose a robustness analysis method based on intra-community connectivity, aiming to optimize transport system protection. De Bona et al. [38] employed network simplification by removing low-degree nodes to retain public transport network backbones, revealing the significance of hub-hub connections and small-world properties. Wei et al. [39] examined the bus route network spatial characteristics, uncovering the impact of administrative divisions on public transport integration. Yang and An [40] constructed a multi-subnetwork complex network model to evaluate urban public transport resilience under extreme weather, analyzing robustness variations via cascading failure simulations. Martín et al. [41] proposed an accessibility-based framework to identify key road netwoek nodes, assessing resilience under various segment disruptions.

Despite the notable advancements of topology-based methods in key node identification, most of reported approaches rely on predefined and static structural metrics. As a result, most approaches are used to capture nonlinear interactions, dynamic propagation behaviors, and complex dependencies among nodes in large-scale transportation networks. Moreover, the reliance on human experience limits the adaptability of the above methods to heterogeneous data, evolving network conditions, highlighting the need for a more flexible learning-based framework.

2.2. Deep learning-based methods

Deep learning, particularly GNN, has recently emerged as a powerful approach for key node identification, demonstrating notable advantages over traditional methods. Unlike topology-based methods, deep learning approaches can automatically learn complex feature representations and integrate multi-dimensional data, including spatiotemporal information and external environmental factors, to achieve more accurate identification. [42] In the context of transportation networks, these methods have spurred distinctive research directions and are increasingly being applied to large-scale, complex systems. Key nodes in complex transportation networks are typically influenced by dynamic traffic flows and spatiotemporal dependencies. Huang et al. [43] proposed a model combining GAT and long short-term memory networks to capture dynamic road interactions and identify key transportation links based on spatiotemporal dependencies. Similarly, Chen et al. [44] introduced MetroGCN, which integrates multi-graph representation and spatiotemporal attention mechanisms to enhance key node prediction accuracy. Research leveraging GNNs has further demonstrated the crucial role of key nodes in predicting network-wide traffic states. Cui et al. [45] proposed KGCGRN-CN, a graph convolutional gated regression network, which integrates network-level and key-node-level spatial features for short-term traffic state prediction, significantly improving prediction accuracy in complex transportation networks. For the quantitative assessment of key nodes, Liu et al. [46] proposed NIE-GAT, which is a GAT-based node importance evaluation method. Applied to inter-domain routing networks, it effectively improved both computational efficiency and accuracy in identifying key nodes. Zhang et al. [47] introduced GATC and DeepCut, combining GAT with normalized cut methods. These approaches are designed for optimizing large-scale transportation networks and segmenting critical areas, thereby enhancing key node identification capabilities. More recently, hybrid methods combining GNNs with other deep learning models have emerged as a significant trend in this field. For example, Zhang et al. [48] proposed BTC-GATs, integrating bidirectional attention, temporal convolutional networks for multiscale features, and graph attention networks for spatial aggregation, to enable efficient key-node identification and traffic monitoring.

Compared to traditional topology-based methods, deep learning-based approaches can automatically learn complex feature representations and process dynamic information, such as spatiotemporal dependencies. However, existing deep

learning-based methods still have some limitations, including limited interpretability, prone to overfitting, and challenges in scaling up to large-scale networks. Additionally many methods focus on learning a single type of feature representation, which may limit their ability to fully utilize heterogeneous network information.

In summary, although existing topology-based and deep learning-based methods have achieved encouraging results in key node identification, there are still some limitations in jointly modeling information, dynamic propagation patterns, and maintaining robustness in different network scenarios. A unified framework is required for integrating network topology, node attributes, and the interactions within a learning-based modeling paradigm. Therefore, this paper proposes a KeyGAM-GCN to effectively fuse multi-source information in complex transportation networks for key node identification with robustness and scalability.

3. Proposed methodology

3.1. Framework of KeyGAM-GCN

KeyGAM-GCN is a novel model for key node identification, and the overall framework of KeyGAM-GCN is shown in Figure 1. The proposed method is used to analyze the key nodes in complex transportation networks with a deep-learning based way, and four key modules of the proposed method are summarized as follows. (1) multi-perspective graph construction, (2) multi-channel graph convolution for feature extraction, (3) gated attention-based feature fusion, and (4) key node prediction. Specifically, deep graph neural networks are leveraged to jointly learn from network topology and node attribute features. To incorporate heterogeneous information sources, structural graph, attribute graph, and structure-attribute fusion graph are used to capture the node characteristics from a different perspective.

The multi-channel GCN module can fuse feature in different layers, capture multi-scale information and preserve essential information by dealing with structural graph, attribute graph, and structure–attribute fusion graph. Specifically, the structural graph encodes the topological connectivity among nodes, which reflect the physical or logical structure of the transportation network; the attribute graph is constructed based on node attribute similarity, which can capture the functional or operational correlations; and the structure–attribute fusion graph jointly integrates topological connections and attribute information to model their interactions.

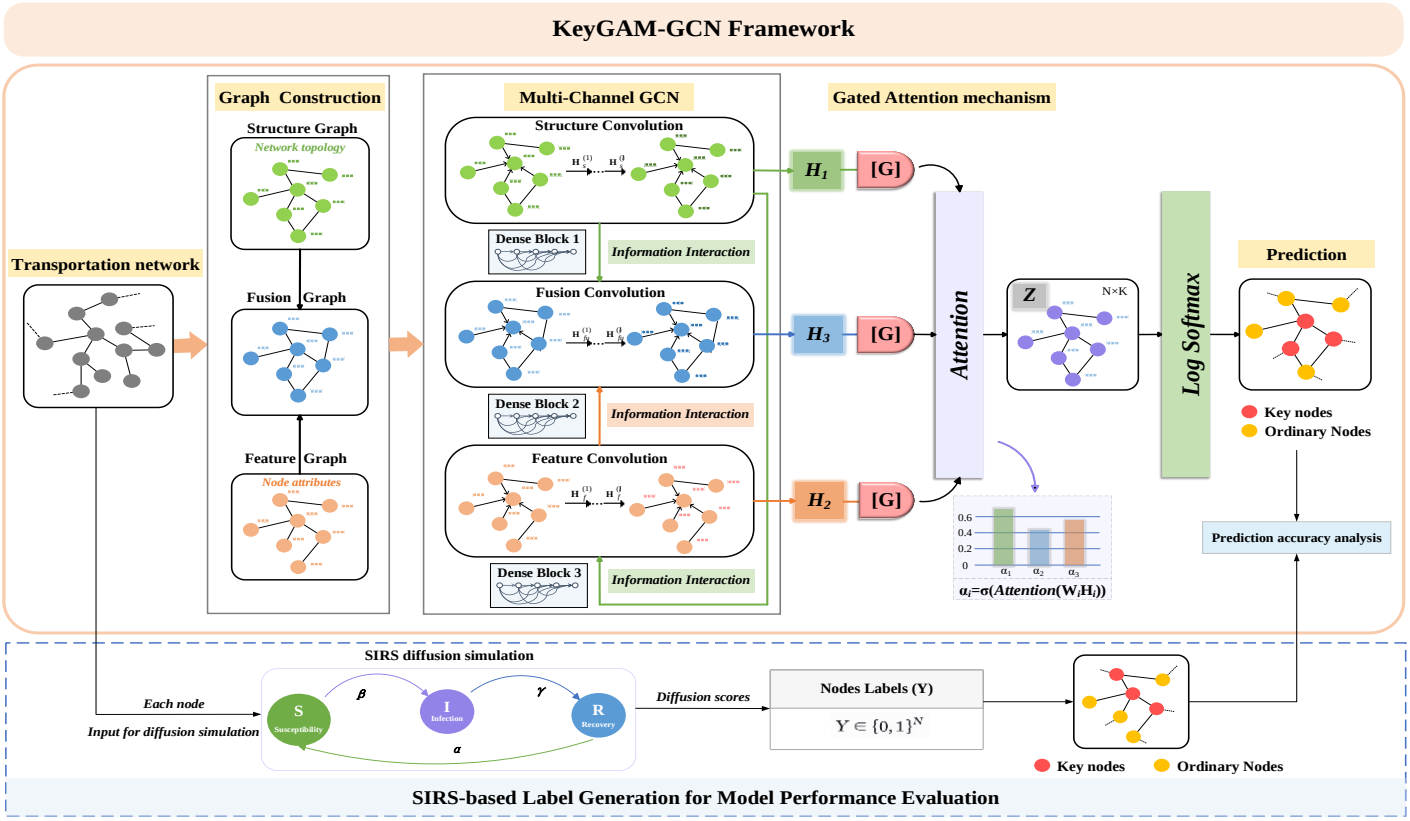

Figure 1. The framework of KeyGAM-GCN for key node identification.

After generating node representations from the three channels, KeyGAM-GCN employs a gated attention mechanism to dynamically fuse the outputs. This mechanism employs learnable gating vectors to adaptively assign importance weights to each channel, allowing the model to selectively emphasize the most relevant features for different node types, thereby enhancing its capability to identify key nodes. The resulting fused node representations are processed through a fully connected layer, and the probability of each node being a key node is output via the Log Softmax function.

Addressing the significant class imbalance inherent in key node identification tasks, KeyGAM-GCN is trained using weighted binary cross-entropy loss, augmented by focal loss to accord greater emphasis to hard-to-classify samples. This dual-loss strategy significantly improves the model's accuracy in identifying the minority class of key nodes. The framework includes the label generation through simulation, graph construction, multi-channel feature extraction and fusion, and node prediction. The model is optimized end-to-end, delivering an efficient and highly scalable solution for key node identification.

3.2. KeyGAM-GCN model

KeyGAM-GCN Model uses the multi-channel GCN module to extract high-level feature representations from the structure graph, attribute graph, and fusion graph, and GAM is used to adaptively adjust weights and fuse these multi-channel features, ultimately outputting the probability of node importance to identify the key nodes.

As illustrated in Figure 1, the overall framework of the model consists of four main components: the input module, the multi-channel graph convolution feature extraction module, the gated attention fusion module, and the output prediction module.

(1) Graph construction in the input module

Complex networks serve as mathematical abstractions for representing real-world complex systems and are typically modeled as a graph structure $G(\boldsymbol{V}, \boldsymbol{E})$, where the set of nodes $\boldsymbol{V}$ represents the fundamental components of the system, and the set of edges E characterizes the interactions or connections between these components. The model input includes the node feature matrix $\boldsymbol{X}$ and the normalized adjacency matrix $\widetilde{\boldsymbol{A}}$. The node feature matrix $\boldsymbol{X}_f \in \boldsymbol{R}^{N\times F}$ represents the attributes of nodes, where the feature dimension **F** is constructed from five categories of network properties. The normalized adjacency matrix $\widetilde{\boldsymbol{A}} \in \boldsymbol{R}^{N\times N}$ encodes the structural relationships between nodes. The node feature matrix **X** is composed of five classical network structural metrics: degree centrality, betweenness centrality, closeness centrality, clustering coefficient, and K-shell value, all of which are standardized.

To enhance the model's capacity to express multi-perspective information, KeyGAM-GCN constructs three types of subgraphs: the structure graph A, the attribute graph (based solely on **X**), and the structure-attibute fusion graph (jointly modeled using both **A** and **X**). These subgraphs are used to extract node representations from different perspectives.

(2) Multi-channel graph convolution feature extraction module

To effectively capture structural information, node attributes, and their fused representations, the hidden layers of KeyGAM-GCN adopt a three-step parallel graph convolution structure. Each convolution unit independently extracts features from distinct subspaces, while cross-layer feature fusion and a gated attention mechanism are incorporated at each layer. Throughout this process, each convolution layer not only receives the input features from the current layer but also recursively integrates the output features from previous layers, thereby enabling deep cross-layer feature fusion. This design facilitates the effective capture of multi-scale node representations. Specifically, the process of feature propagation and fusion in the hidden layers is formulated as follows.

$$\begin{aligned} \boldsymbol{H}_1 &= \sigma\left(\widetilde{\boldsymbol{A}}\boldsymbol{X}_s\boldsymbol{W}_1\right) \\ \boldsymbol{H}_2 &= \sigma\left(\widetilde{\boldsymbol{A}}\left(\boldsymbol{X}_f + \boldsymbol{H}_1\right)\boldsymbol{W}_2\right) \\ \boldsymbol{H}_3 &= \sigma(\widetilde{\boldsymbol{A}}(\boldsymbol{X}_{fu} + \boldsymbol{H}_1 + \boldsymbol{H}_2)\boldsymbol{W}_3) \end{aligned} \tag{1}$$

where $\boldsymbol{H}_1$, $\boldsymbol{H}_2$, and $\boldsymbol{H}_3$ denote the output features of the structure, attribute, and structure-attribute graph convolution layers, respectively; while $\boldsymbol{W}_1$, $\boldsymbol{W}_2$, and $\boldsymbol{W}_3$ represent the corresponding learnable weight matrices, respectively; The function $\sigma(\cdot)$ denotes the activation function; $\boldsymbol{X}_s$ corresponds to the structural feature matrix; $\boldsymbol{X}_{fu}$ represents the fused feature matrix.

(3) Gated attention fusion module

To integrate the extracted features from the three channels and enhance the discrimination capability, GAM is used by learnable gating vectors to weigh the contributions of each

channel's output. The computation for each gating unit is defined as follows.

$$\omega_i = \sigma(\boldsymbol{W}_g \boldsymbol{H}_i), i = 1,2,3 \quad (2)$$

where ω_i represents the weighting coefficient for the feature representation obtained from the i-th convolutional step; while $\boldsymbol{W}_g$ denotes the learnable gating weight matrix.

Finally, the comprehensive node representation $\boldsymbol{Z}$ is obtained by performing a weighted fusion of the multi-level features according to their respective weights:

$$\boldsymbol{Z} = \omega_1 \boldsymbol{H}_1 + \omega_2 \boldsymbol{H}_2 + \omega_3 \boldsymbol{H}_3 \quad (3)$$

(4) Output prediction module

The output layer of the model directly generates unnormalized prediction values (logits) for each node, which are then mapped into binary probabilities of node importance through the Sigmoid function. To optimize the model parameters, this study employs the Binary Cross-Entropy with Logits Loss (BCEWithLogitsLoss) as the training objective, which is defined as follows:

$$\mathcal{L}_{BCE-log\,its} = -\frac{1}{N}\sum_{i=1}^{N} [y_i \cdot log\,\sigma(z_i) + (1-y_i) \cdot log(1-\sigma(z_i))] \quad (4)$$

where N denotes the total number of nodes, y_i represents the ground truth label; z_i is the model output (logit), and $\sigma(z_i)$ denotes the Sigmoid function.

The process of learning new node features is detailed in Algorithm 1.

From a computational perspective, the complexity of KeyGAM-GCN is primarily dominated by the multi-channel graph convolution layers and the gated attention fusion module. For a standard graph convolution operation on a sparse graph, the time complexity of a single forward pass can be expressed as $O(|\boldsymbol{E}| \cdot |\boldsymbol{F}| + |\boldsymbol{V}| \cdot \boldsymbol{F}^2)$,where $|\boldsymbol{V}|$ and $|\boldsymbol{E}|$ denote the numbers of nodes and edges, respectively, and $|\boldsymbol{F}|$ represents the feature dimension. In KeyGAM-GCN, multiple graph convolution channels are employed to capture node representations from different structural views; however, these channels operate in parallel and do not introduce higher-order complexity. The gated attention mechanism mainly involves node-wise linear transformations and weighted feature aggregation, whose computational cost remains in the same order as that of graph convolution. As a result, the overall time complexity of KeyGAM-GCN remains within the same asymptotic order as conventional GCN-based models, indicating that the enhanced representation capability is achieved without introducing prohibitive computational overhead, and the proposed framework is suitable for application to medium- and large-scale transportation networks.

Algorithm 1 Feature Update in KeyGAM-GCN

Inputs: Network G, Node feature matrix $\boldsymbol{X}$, Weight matrices $\boldsymbol{W_1}$, $\boldsymbol{W_2}$, $\boldsymbol{W_3}$;
Adjacency matrices A_{struct}, $\boldsymbol{A}_{attr}$, $\boldsymbol{A}_{fusion}$;
Gating mechanism *Gate*(), Attention mechanism *Attn*();
Output: Updated feature matrix of nodes $\boldsymbol{Z}$
1: Initialize KeyGAM-GCN model parameters;
2: **For** *each node i* in G **do**
3: $x_i \leftarrow$ X [i];
4: Compute hidden representations via multi-channel GCNs by Eq.(1):
5: $\boldsymbol{H}_1[i] \leftarrow \sigma(\sum_{j\in N(i)} \boldsymbol{A}_{struct}[i][j] \cdot x_j \cdot \boldsymbol{W}_1[i])$;
6: $\boldsymbol{H}_2[i] \leftarrow \sigma(\sum_{j\in N(i)} \boldsymbol{A}_{attr}[i][j] \cdot x_j \cdot \boldsymbol{W}_2[i])$;
7: $\boldsymbol{H}_3[i] \leftarrow \sigma(\sum_{j\in N(i)} \boldsymbol{A}_{fusion}[i][j] \cdot x_j \cdot \boldsymbol{W}_3[i])$;
8: Compute gated attention weights for each branch using Eq.(2):
9: $\omega_1 \leftarrow$ softmax(Gate($\boldsymbol{H}_1$)· $\boldsymbol{W}_g$);
10: $\omega_2 \leftarrow$ softmax(Gate($\boldsymbol{H}_2$)· $\boldsymbol{W}_g$);
11: $\omega_3 \leftarrow$ softmax(Gate($\boldsymbol{H}_3$)· $\boldsymbol{W}_g$);
12: Fuse multi-channel outputs using weighted sum using Eq.(3):
13: $\boldsymbol{Z} \leftarrow$ □$_1$□$_1$ + □$_2$□$_2$ + □$_3$□$_3$;
14: **End for**
15: $\boldsymbol{Z} \leftarrow$ Stack all z_i;
16: Compute output prediction:
17: $\hat{y} \leftarrow$ log_softmax($\boldsymbol{Z}$);
18: Compute lossusing Eq.(4):
19: $\mathcal{L}_{BCE-log\,its} = -\frac{1}{N}\sum_{i=1}^{N}[y_i \cdot log\,\sigma(z_i) + (1-y_i) \cdot log(1-\sigma(z_i))]$
20: **Return** $\boldsymbol{Z}$, $\mathcal{L}$

3.3. SIRS - based offline lable generation for model performance evaluation

For the current transportation datasets, it is hard to mark the ground truth labels for key nodes in real-world complex networks. Consequently, researchers frequently employ epidemic-spreading models to simulate the node information diffusion processes according to the diseases propagation, thereby indirectly assessing the improtance of nodes. The classic Susceptible-Infected-Recovered (SIR) model is widely used for static diffusion simulations [49], which cannot inadequately capture the recurrent state transitions common in real-world scenarios. Unlike the SIR model, SIRS permits

recovered nodes to revert to a susceptible state, thereby facilitating the evaluation of long-term diffusion capabilities across multiple propagation cycles. For the transportaiton network, the recovery strategies after some emergency events are often considered in practical transportation systems. So SIRS model is more suitable for simulating the cyclic propagation process within the transportation network under dynamic spreading environments.

To generate the labels for model evaluation in the key node identification task, multiple rounds of SIRS-based simulation are conducted. In each round, a single node is randomly selected as the initial infected source, and the infection process is simulated over a predeterined number of time steps. The average number of nodes infected by each seed node across multiple simulations is recorded to evaluate its diffusion capability score. To mitigate stochasticity and the impact of local structural variations, the mean score from repeated experiments is utilized for each node. So the importance of nodes are ranked in descending order according to the diffusion score. Following common practice in key node identification and influence analysis, a fixed-ratio strategy is used to define the top 5% nodes with the highest diffusion score as the key nodes [21]. Moreover, the proportion has been used to generate stable and discriminative ranking results in complex networks [49]. Therefore, 5% is set as a threshold to distinguish the key nodes and non-key nodes.

The SIRS model categorizes nodes into three dynamic states: susceptible nodes (*S*), infected nodes (*I*), and recovered nodes (*R*). The transitions between these states are formulated by the following differential equations.

$$\begin{cases} \frac{dS}{dt} = -\beta SI + \alpha R \\ \frac{dI}{dt} = \beta SI - \gamma I \\ \frac{dR}{dt} = \gamma I - \alpha R \end{cases} \quad (5)$$

where *S*, *I*, and *R* represent the proportions of susceptible, infected, and recovered nodes in the network; β denotes the infection probability; γ represents the recovery probability, and α is the probability when a recovered node is susceptible again. Specially, β reflects the propagation speed of congestion, disruptions, or operational disturbances in transportation network; γ characterizes the restoration ability of transportation system after the emergency events, which is related to the recovery strategy; and α captures the vulnerability of recovered nodes after the recurrent congestion or secondary disturbances.

According to the heterogeneous mean-field theory [50], the epidemic threshold of the SIRS model, which determines whether a widespread outbreak will occur, can be approximated as Equation 2.

$$\lambda_c = \frac{<k>}{<k^2>-<k>} \quad (6)$$

where $< k >$ represents the average degree of the network. To ensure that all networks remain in a transmissible state and exhibit sufficient differentiation among node influences, the target effective infection rate was set to satisfy $\lambda > \lambda c$.

Ten real-world transportation networks with average degrees ranging from 2 to 12 were analyzed. To ensure that the propagation process remains in a metastable state, allowing for effective but non-saturating infection γ is fixed at 0.1 and α at 0.05, while β denotes is adjusted according to the average degree of each network such that the effective infection rate $\lambda = \beta/\gamma$ is adjust approximately 5-10 times the corresponding threshold λ_c. Specifically, β denotes was set to around 0.3-0.5 for sparse networks ($< k >$≈2-4) and 0.6-0.8 for denser networks ($< k >$≈8-12).

4. Experimental setup

4.1. Datasets

To verify the accuracy and generalizability of the KeyGAM-GCN model, nine real-world transportation datasets are selected, which are ordered by network size from the smallest to the largest. All networks are regarded as undirected and unweighted graphs through the unified preprocessing procedures. Specifically, bidirectional connections are established by symmetrizing the edge directions for the datasets with directed edges, such that an edge is retained if it exists in either direction. For weighted edges in a network, the original weights are discarded and all edges are regarded as binary connections, indicating the existence of a link between two nodes. This preprocessing strategy can ensure fair comparison across heterogeneous transportation datasets and to reduce the influence of inconsistent or domain-specific weight definitions.

- inf-USAir97: a dataset modeling the USAir97 airline network, which represents domestic flight connections in the United States.
- Anaheim Network: a road transportation network of

Anaheim, used for traffic flow analysis.

- London Public Transport Network: a dataset representing the public transport network of London, including stations and routes.
- Barcelona Network: a dataset representing the urban transportation network of Barcelona, used for mobility analysis.
- Winnipeg Network: a road network dataset of Winnipeg.
- inf-openflights network: a dataset modeling the global airline network, covering airports and flight routes.
- Gold Coast Network: a dataset representing the road transportation network of Gold Coast, Australia.
- Austin Network: a dataset modeling the traffic network of Austin, Texas, used for congestion analysis.
- Philadelphia Network: a dataset representing the road transportation network of Philadelphia.

Table 1 presents some statistical characteristics of nine real-world networks, which represent network representations of different transportation systems with varying topological structures and features.

Table 1. The statistical properties of the 9 real networks

Networks	n	m	$< k >$	$k_{\max}$	c	d
Inf-USAir97 Network	332	2127	12.81	139	0.6252	0.0387
Anaheim Network	416	634	3.04	7	0.1076	0.0073
London Public Transport Network	653	976	2.48	14	0.0278	0.0038
Winnipeg Network	948	1384	2.91	5	0.0114	0.0031
Barcelona Network	1020	2522	3.86	16	0.0902	0.0041
Inf-openflights Network	2939	15677	10.67	242	0.4526	0.0036
Gold Coast Network	4807	5952	2.48	6	0.0417	0.0005
Austin Network	7388	10591	2.86	7	0.0121	0.0004
Philadelphia Network	13389	21246	3.17	5	0.0146	0.0002

Notes: n denotes the number of nodes, m represents the number of edges, and $<k>$ is the average degree of the network. k_{max} denotes the maximum degree, c is the average clustering coefficient, and d represents the network density, which measures the ratio of actual edges to the total possible edges in the network.

4.2. Evaluation metrics

Kendall's Tau: Based on the propagation capability of nodes within the network, a descending ranking list of node importance is generated using the SIRS model. The Kendall's tau coefficient (τ) is employed to assess the correlation between the ranking list obtained from a given importance metric and the actual ranking derived from the SIRS model [51]. A higher τ value indicates a stronger correlation between the two ranking lists, implying greater accuracy in the importance estimation. When Kendall's tau coefficient approaches one, the ranking results are more precise, demonstrating the effectiveness of the method in identifying key nodes.

$$\boldsymbol{\tau} = \frac{\mathbf{2}(\boldsymbol{n_c}-\boldsymbol{n_i})}{\boldsymbol{n}(\boldsymbol{n}-\mathbf{1})} \tag{7}$$

where $\boldsymbol{n_c}$ and $\boldsymbol{n_i}$ represent the number of concordant and discordant pairs, respectively; $\boldsymbol{n}$ denotes the total number of paired comparisons. The Kendall's tau coefficient τ ranges from [-1, 1]. Ideally, if $\tau = 1$, the ranking list produced by the degree centrality is perfectly consistent with the ranking obtained from the actual propagation process.

NDCG: Normalized Discounted Cumulative Gain (NDCG) is a classical metric for assessing ranking quality by jointly considering the relevance scores of ranked elements and their positions, which is commonly used in recommendation systems [52] and node importance ranking [53]. NDCG can assign higher scores to the top nodes through a position discount factor. In key node identification tasks, the primary goal is to correctly prioritize the most influential nodes rather than to achieve a perfect global ordering, which makes NDCG particularly suitable for evaluating ranking effectiveness.

$$NDCG@K = \frac{DCG@K}{IDCG@K} \tag{8}$$

where K represents the length of the ranking list; DCG denotes the discounted cumulative gain, and IDCG corresponds to the ideal discounted cumulative gain. The bounded range of NDCG ensures that higher values signify rankings that more accurately align with the optimal order.

ISE: Influence Spread Error (ISE) quantifies the discrepancy between the influence spread of the predicted key node set and that of the ground truth key node set in real diffusion simulations. The calculation formula is as follows.

$$ISE = \frac{|I_{ture} - I_{pred}|}{I_{ture}} \tag{9}$$

where I_{ture} represents the average infection scale of the ground truth key nodes; and I_{pred} denotes the average infection scale of the predicted key nodes. A smaller ISE value indicates better performance, with an ideal value of 0 signifying that the predicted key nodes exhibit the same diffusion capability as the true key nodes.

4.3. Ablation study

To analyze the contribution of different modules in KeyGAM-GCN, the ablation experiments are implemented. Specifically, we progressively introduce key modules into the model to assess their impact on key node identification performance. The ablation study consists of the following comparative settings:

- MC-GCN: The baseline model, which is a multi-channel GCN without any additional modules.
- MC-GCN(+II): This variant incorporates the information interaction module.
- MC-GCN(+GA): This variant adds the gate-attention mechanism.
- MC-GCN(+II&GA): This variant combines both the information interaction module and the gate-attention mechanism.

Table 2 presents the results of the ablation experiments conducted on nine real-world transportation networks. The experimental results demonstrate that the baseline MC-GCN model exhibits stable benchmark performance across all networks (average ACC = 0.7815), confirming the fundamental capability of the multi-channel architecture in capturing network topological features. The progressive incorporation of the information interaction module (II) and the gate-attention mechanism (GA) significantly enhances the model's ability to identify key nodes. Specifically, the introduction of the information interaction module (II) increases the model's average accuracy to 0.8024, with a notable 8.9% improvement in the τ coefficient on the inf-USAir97 network, indicating that this module strengthens feature interaction and enables the model to leverage network structure information more effectively through cross-layer feature fusion. Meanwhile, the addition of the gate-attention mechanism (+GA) further improves performance, demonstrating a more pronounced advantage in feature fusion by increasing the average ACC to 0.8546. Notably, in the London Public Transport Network, the F1-score improves by 21.4%, suggesting that this mechanism effectively adjusts the weight distribution among different feature channels, thereby enhancing the accuracy of key node identification. It is particularly noteworthy that the combination of the information interaction module and the gate-attention. Mechanism (+II & GA) results in significant performance gains, achieving the best results across nearly all datasets (average ACC = 0.9014, F1 = 0.8976, τ = 0.7869). For instance, in the Anaheim Network, ACC increases to 0.9237, F1-score reaches 0.9216, and τ improves to 0.8492, all showing substantial gains over the baseline model. This demonstrates that the integration of both modules further strengthens feature extraction and fusion capabilities, leading to improved model stability and generalization. Overall, the ablation study results strongly validate the effectiveness of the proposed enhancements in the KeyGAM-GCN model for key node identification tasks, confirming that the synergy between information interaction and the gate-attention mechanism significantly enhances the model's representational power, enabling superior performance across diverse network scenarios.

To further illustrate the impact of each module, we present three contribution enhancement heatmaps in Figure 2, which depict the relative gains in accuracy (ACC), F1-score, and Kendall's Tau (τ) compared to the baseline model MC-GCN across all datasets. These heatmaps provide an intuitive visualization of how the information interaction module (+II), the gated attention mechanism (+GA), and their combination (+II & GA) progressively enhance model performance.

From the overall improvement trends, all three model variants contribute to performance enhancement across most datasets and evaluation metrics, demonstrating the effectiveness of the proposed improvements to MC-GCN. The ACC contribution enhancement heatmap clearly shows that both the +II and +GA modules significantly improve performance across all datasets, with their combination (+II & GA) yielding the most substantial gains. The F1 contribution enhancement heatmap reveals a similar pattern, further confirming the effectiveness of these modules. Meanwhile, the τ contribution enhancement heatmap highlights the broader impact of our approach, showing that the proposed modules not only enhance classification performance but also improve the ranking quality of identified key nodes.

Table 2. The ablation study results on nine datasets.

Network	Metric	MC-GCN	+II	+GA	+II&GA
inf-USAir97 network	ACC	0.8984	0.9401	0.9418	**0.9424**
	F1	0.8859	0.9372	0.9100	**0.9384**
	τ	0.8135	0.8861	0.8873	**0.8907**
Anaheim Network	ACC	0.7780	0.8105	0.8562	**0.9237**
	F1	0.7934	0.8123	0.8408	**0.9216**
	τ	0.7791	0.7961	0.8141	**0.8492**
London Public Transport Network	ACC	0.7183	0.8084	0.8665	**0.9012**
	F1	0.7082	0.8059	0.8594	**0.8942**
	τ	0.4370	0.6169	0.7347	**0.8064**
Winnipeg Network	ACC	0.7517	0.7661	0.8604	**0.8886**
	F1	0.7442	0.7740	0.8666	**0.8862**
	τ	0.5062	0.5348	0.7256	**0.7775**
Barcelona Network	ACC	0.7533	0.7555	0.8268	**0.8292**
	F1	0.7534	0.7636	0.8308	**0.8324**
	τ	0.5068	0.5128	0.6558	**0.6588**
inf-openflights Network	ACC	0.9076	0.9138	0.9063	**0.9257**
	F1	0.9041	0.9100	0.8995	**0.9249**
	τ	0.8185	0.8319	0.8229	**0.8523**
Gold Coast Network	ACC	0.8000	0.8350	0.8341	**0.9111**
	F1	0.8039	0.8320	0.8274	**0.9080**
	τ	0.6005	0.6704	0.6710	**0.8249**
Austin Network	ACC	0.6407	0.7543	0.7764	**0.8862**
	F1	0.6214	0.7669	0.7648	**0.8730**
	τ	0.4827	0.5132	0.5544	**0.7866**
Philadelphia Network	ACC	0.7874	0.8399	0.8268	**0.9063**
	F1	0.7906	0.8451	0.8324	**0.8995**
	τ	0.5755	0.6797	0.6558	**0.8229**

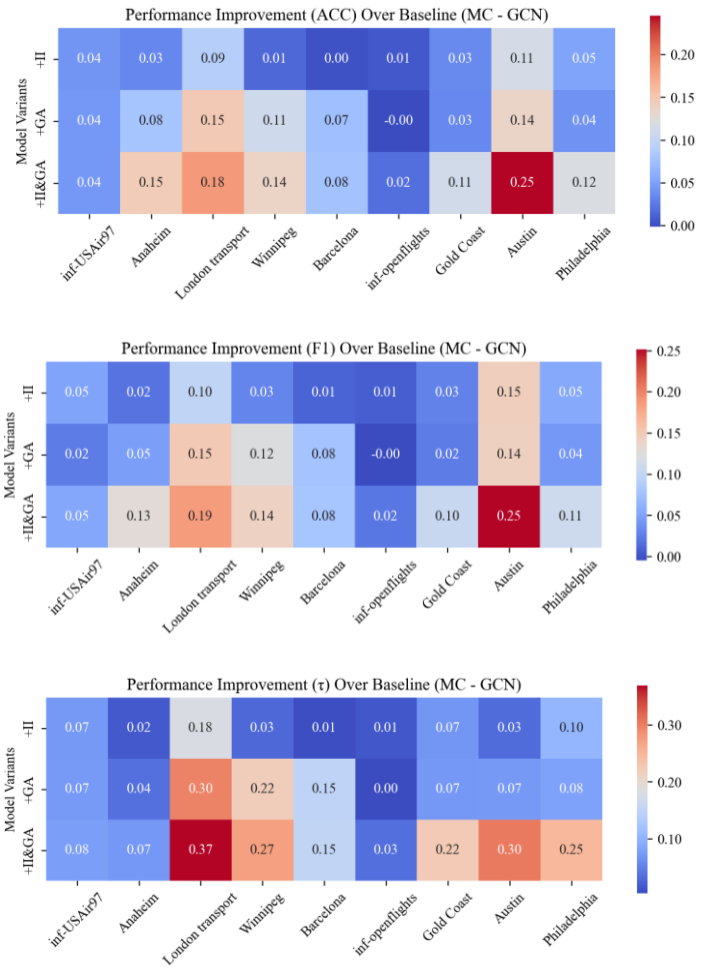

Figure 2. The contributions of the three key modules in KeyGAM-GCN.

4.4. Performance analysis for KeyGAM-GCN

To comprehensively evaluate the performance of KeyGAM-GCN in key node identification tasks, we conducted comparative experiments against multiple state-of-the-art

baseline models. These include graph neural network (GNN)-based models such as APPNP [54], MixHop [55], SGC [56], GCN, and GAT, as well as network centrality-based methods, specifically degree centrality (DC) and closeness centrality (CC). In all experiments, we employed Accuracy (ACC), F1-score, and Kendall's Tau (τ) as evaluation metrics to thoroughly assess each model's classification capability and ranking quality.

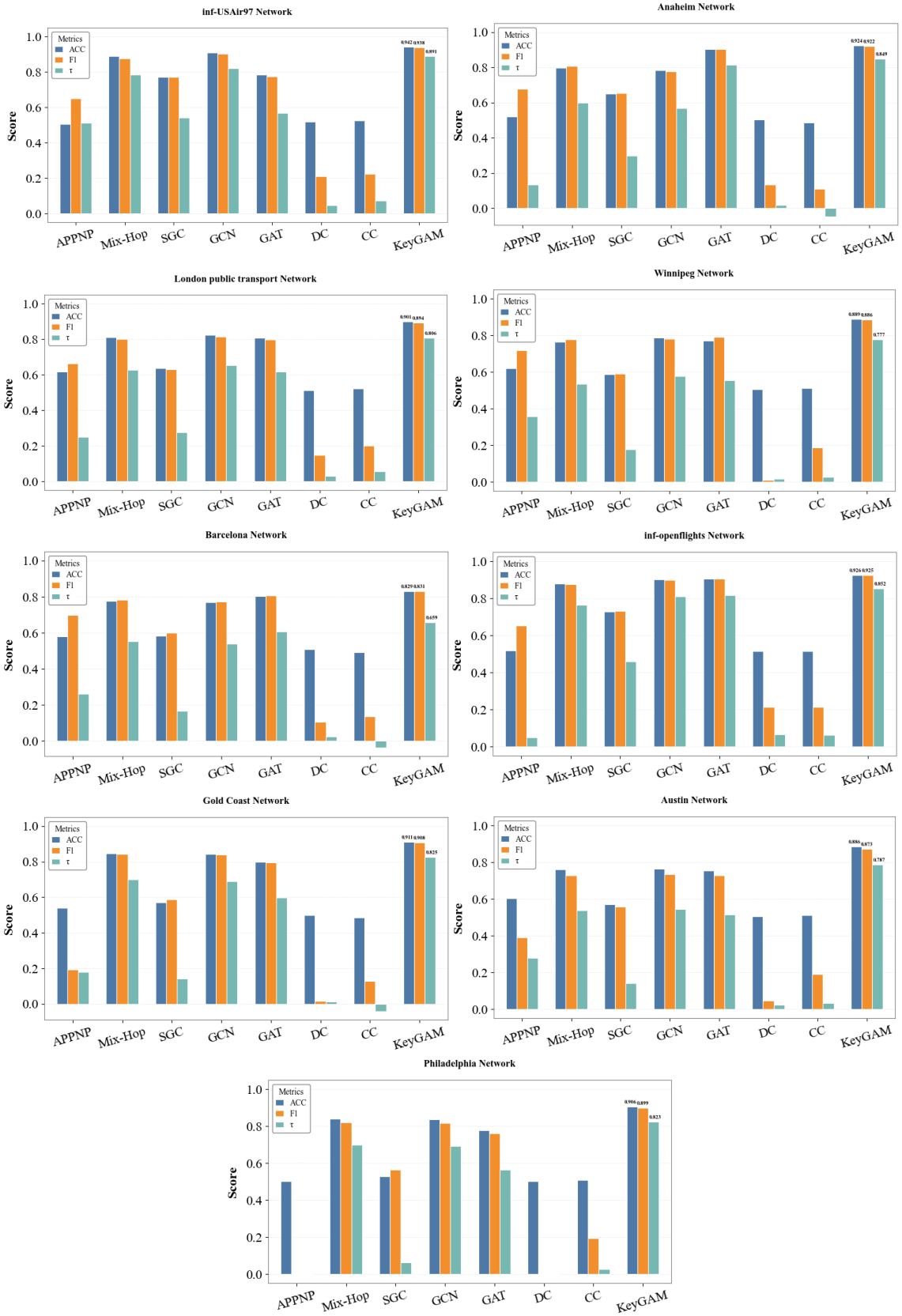

Figure 3. Performance comparison of KeyGAM-GCN and baseline models.

To provide a more intuitive comparison of KeyGAM-GCN with other baseline models across different datasets, we have plotted bar charts illustrating the performance of each model on the three evaluation metrics, as shown in Figure 3. It can be observed that KeyGAM-GCN consistently outperforms all baseline models across all datasets in terms of all three evaluation metrics, demonstrating its superior generalization ability and robustness in key node identification tasks. While mainstream GNN-based models such as GCN, GAT, and MixHop can capture network structural information to a certain extent, their classification performance remains limited due to the lack of specific optimization for key node identification. Although APPNP achieves competitive performance through enhanced information propagation, its ranking capability reflected in the τ metric still lags behind KeyGAM-GCN. SGC offers improved computational efficiency but suffers from reduced capacity, resulting in lower accuracy. In addition, traditional centrality-based methods (DC and CC) perform consistently worse across all datasets, indicating that relying solely on topological features is insufficient for effective key node identification. By contrast, KeyGAM-GCN significantly enhances key node recognition and maintains stable superiority across diverse networks.

5. Case study: Beijing subway network

In this section, we presents a case study of the Beijing Subway network, systematically evaluating the performance of the KeyGAM-GCN model in the task of key node identification within real-world transportation networks. First, we compare the classification performance of KeyGAM-GCN with multiple baseline models to assess its predictive accuracy and ranking consistency. Second, we compute the NDCG at different values of K to evaluate the effectiveness of each model in ranking key nodes. Furthermore, we analyze the variation in key node ISE values as K% changes, providing insights into the impact of different models on the efficiency of information propagation. Finally, we conduct a sensitivity analysis by adjusting the epidemic dynamics parameters to examine the model's robustness and ranking consistency in network propagation processes.

The Beijing Subway network, serving as the experimental dataset, consists of 401 stations (nodes) and 478 edges, forming a complex transportation system. The basic topological properties of the network are as follows. n = 401, m = 478, $\langle k \rangle$ = 2.41, k_{max} = 6, c = 0.0063, and d = 0.0059. Specifically, the station information and line data of Beijing Subway is obtained by the Amap API, and the subway network topology is constructed by NetworkX. In the transportation network, each station (node) represents a subway station, while the rail connections (edges) between stations represent direct transfer relationships between adjacent stations. Furthermore, the constructed NetworkX graph is we converted into PyTorch Geometric (PyG) format to accommodate graph neural network (GNN)-based model training and experimental analysis. The topology of the Beijing Subway network is shown in Figure 4.

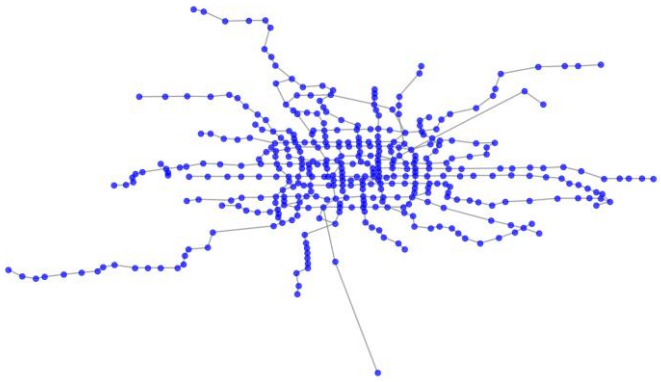

Figure 4. The topological structure of Beijing Subway.

5.1. Model performance analysis

The performance evaluation of KeyGAM-GCN is performed by comparing with six baseline models on Beijing subway network. The experimental setup employed propagation dynamics parameters set to β =0.5, γ =0.1,and α =0.05,with node importance labels generated through 1,000 iterations of the SIRS model simulation. As shown in Table 3, KeyGAM-GCN consistently demonstrates a significant advantage across multiple performance metrics.

Table 3 presents a detailed comparison of model performance. The results indicate that KeyGAM-GCN significantly outperforms other methods in terms of accuracy (ACC) and F1-score. Notably, while APPNP and GCN achieve score. Notably, while APPNP and GCN achieve slightly higher recall than KeyGAM-GCN, the superior precision and F1-score of KeyGAM-GCN suggest that its predictions are more reliable. From a practical application perspective, the high Kendall's Tau

(τ) value of KeyGAM-GCN is particularly valuable. Analysis shows that the top 10% of key stations identified by KeyGAM-GCN account for 89.5% of the system's potential propagation risk, which is crucial for designing precise prevention and control strategies.

Table 3. Performance comparison of KeyGAM-GCN and baseline methods.

Method	ACC	F1	Recall	τ
APPNP	0.7920	0.8095	0.8867	0.5950
Mix-Hop	0.8071	0.8157	0.8563	0.6174
SGC	0.7947	0.8026	0.8370	0.5917
GCN	0.8512	0.8532	0.8674	0.7028
GAT	0.8429	0.8398	0.8259	0.6862
DC	0.5013	0.0320	0.0165	0.0003
CC	0.5371	0.2363	0.1436	0.1166
KeyGAM	**0.9201**	**0.9152**	**0.8646**	**0.8453**

The performance of traditional centrality-based methods provides important insights. Both degree centrality (DC) and closeness centrality (CC) exhibit significantly weaker results. This suggests that in complex systems such as subway networks, relying solely on topological features is insufficient for effectively capturing dynamic propagation characteristics. Additionally, the performance of the GAT model warrants attention. Although its accuracy is relatively high, its recall is lower than that of GCN. Our analysis suggests that this may be due to the attention mechanism overly focusing on a few important neighbors while neglecting the characteristics of global propagation pathways.

5.2. Ranking performance evaluation

To further evaluate the effectiveness of different models in key node ranking tasks, this section analyzes Normalized Discounted Cumulative Gain ($NDCG@K$) performance for various values of K (10, 20, 30, 40, 50). $NDCG@K$ is a crucial metric for assessing the quality of key node ranking, where higher values indicate that the model's ranking is more consistent with the true importance distribution of nodes in terms of propagation risk. To provide an intuitive comparison of ranking performance across different models, we present the $NDCG@K$ curves for each method at different K values, as illustrated in Figure 5.

The $NDCG@K$ of all models increases with K, indicating enhanced ranking stability for larger key node sets, and the relative ranking errors among the top K nodes decrease. The results align with the propagation dynamics of complex networks, and the influence of key nodes often follows a long-tail distribution. The accuracy of the top 10 nodes ranking depends on the overall propagation, and local ranking errors exert a diminishing effect on the global results as K increases, which leads to a gradual increase of $NDCG@K$. Moreover, as shown in Figure 5, KeyGAM-GCN consistently achieves the highest NDCG for K = 10, 20, 30, 40 and 50, which demonstrates the robustness and effectiveness in key node ranking. Furthermore, KeyGAM-GCN maintains a leading position as K increases, reaching an NDCG@50 score of 0.9021, indicating that it can effectively identify key nodes not only within a small subset (K =10) but also across a broader range (K =50). Therefore, the results show that KeyGAM-GCN is well-suited for key nodes identification in diverse transportation networks.

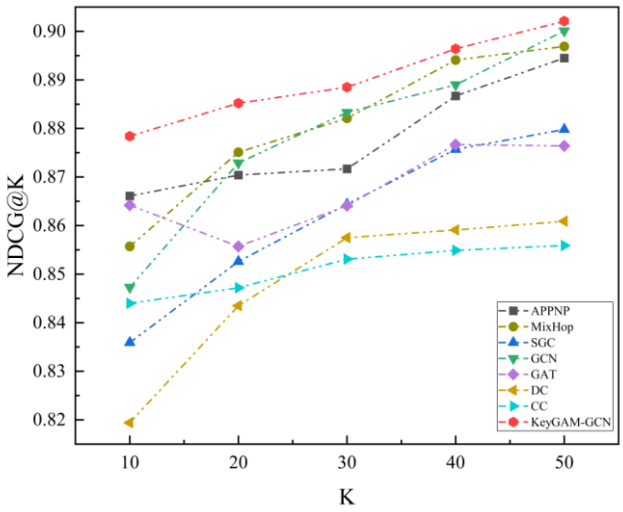

Figure 5. $NDCG@K$ performance curves of seven methods.

The $NDCG@K$ of all models increases with K, indicating enhanced ranking stability for larger key node sets, and the relative ranking errors among the top K nodes decrease. The results align with the propagation dynamics of complex networks, and the influence of key nodes often follows a long-tail distribution. The accuracy of the top 10 nodes ranking depends on the overall propagation, and local ranking errors exert a diminishing effect on the global results as K increases, which leads to a gradual increase of $NDCG@K$. Moreover, as shown in Figure 5, KeyGAM-GCN consistently achieves the highest NDCG for K = 10, 20, 30, 40 and 50, which demonstrates the robustness and effectiveness in key node ranking. Furthermore, KeyGAM-GCN maintains a leading position as K increases, reaching an NDCG@50 score of 0.9021, indicating that it can effectively identify key nodes not

only within a small subset (K =10) but also across a broader range (K =50). Therefore, the results show that KeyGAM-GCN is well-suited for key nodes identification in diverse transportation networks.

5.3. Spreading influence analysis

The Influence Spread Error (ISE) across different coverage proportions (5%, 10%, 15%, 20%, 25%, and 30%) is analyzed to evaluate the effectiveness of various models in key node identification tasks. The ISE can measure the discrepancy between the predicted set of key nodes and the actual influence spread, with lower ISE values indicating a higher alignment between the identified key nodes and the true propagation patterns. The variation of ISE with respect to L % for different methods is illustrated in Figure 6.

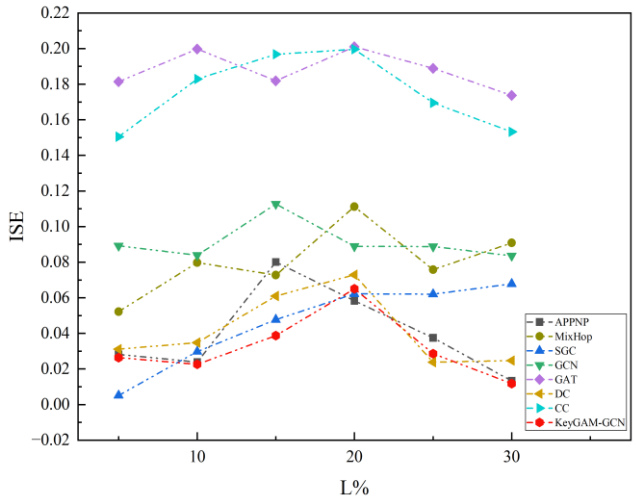

Figure 6. ISE performance curves of eight methods.

From an overall perspective, different methods exhibit distinct trends across various key node proportions. KeyGAM-GCN and APPNP achieve the lowest ISE values when the key node proportion is between 5% and 10%, demonstrating their strong precision in small-scale key node identification tasks. This suggests that these methods effectively prioritize selecting core nodes with the most significant influence on controlling propagation. However, in the 15%-20% key node proportion range, the ISE of most methods, including MixHop and GAT, increases. This rise may be attributed to these models relying more on local structural features at this stage, failing to fully capture global propagation dynamics, and consequently selecting nodes that are structurally important but contribute less to overall influence control. In contrast, KeyGAM-GCN exhibits a relatively smaller increase in ISE within this range, suggesting its superior adaptability across different key node scales.

Notably, at 30% coverage, KeyGAM-GCN attains the lowest overall ISE, indicating that the selected key nodes are effective to cover major propagation pathways and mitigate propagation risk. Additionally, KeyGAM-GCN demonstrates consistently low ISE for all tested key node proportions, with particularly strong performance at 5%, 10%, and 30%. Among these, the 30% key node proportion achieves the lowest ISE, which shows that the identified key node set is sufficient to cover major propagation risks and effectively suppress the network-wide influence spread. Meanwhile, the 10% key node proportion represents the optimal cost-effectiveness balance, which enables the control of 86% of the spread risk with minimal resource investment. Therefore, the KeyGAM-GCN can achieve a bettter performance under different proportions of key nodes in the transportation network.

5.4. Sensitivity analysis

The variations in the Kendall correlation coefficient of different models under varying recovery rates γ and reinfection rate α on the Beijing subway dataset are analyzed. The objective is to evaluate the robustness of KeyGAM-GCN and other methods to changes in epidemic spreading dynamics. Specifically, the γ is set to values ranging from 0.05 to 0.9, and the α varies within the same range. The results are presented as two line charts depicting the Kendall coefficient variations for different methods.

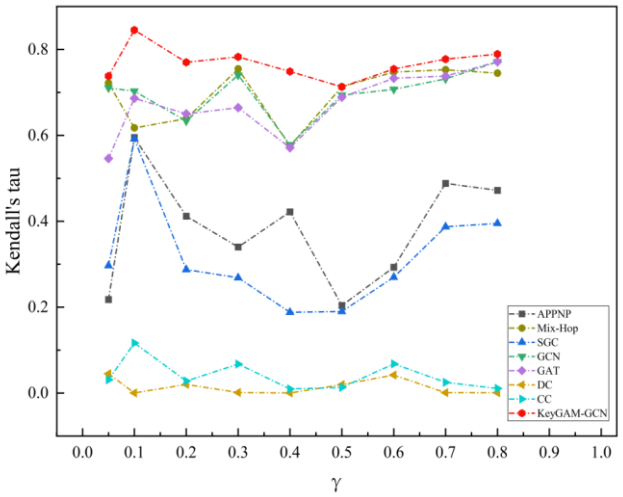

Figure 7. Variation of Kendall's τ coefficient with respect to γ.

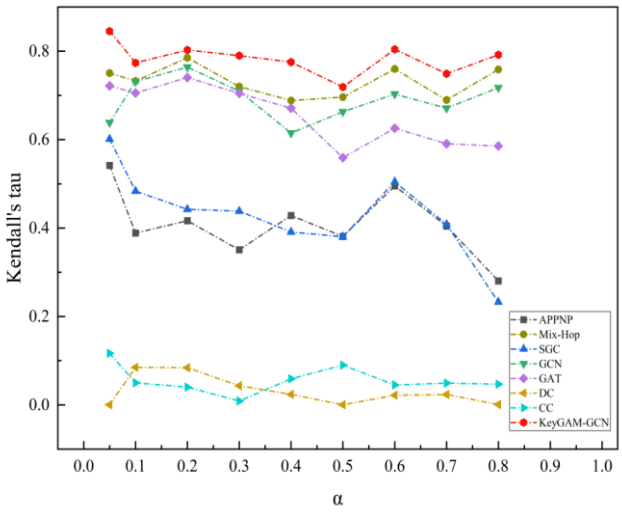

Figure 8. Variation of Kendall's τ coefficient with respect to α.

Figure 7 shows the variations in the Kendall coefficient of different models under changes in the recovery rate. The variation of the recovery rate γ has a significant nonlinear impact on model performance, and the Kendall τ coefficient of all models exhibits a distinct "U-shaped" change as γ increases. When γ is in the medium range of 0.1 to 0.3, all models show a significant performance decline. This U-shaped trend essentially reflects the trade-off between the "memory effect" and "recovery speed" in the epidemic spreading process: lower γ values cause the infection state to persist for a longer period, allowing the system to accumulate more historical information, which facilitates the model's learning of key node features, while higher γ values lead to rapid recovery, causing the network to quickly return to a quasi-steady state, making the influence of key nodes more stable. Under moderate recovery rates, the system is in an unstable dynamic transition process, where key node rankings are more disturbed, leading to a decrease in the Kendall coefficient.

It can be observed that KeyGAM-GCN achieves the highest Kendall coefficient under most values of γ, demonstrating strong adaptability to different recovery rates. At γ=0.1, KeyGAM-GCN achieves the highest Kendall coefficient of 0.8453, indicating that its key node ranking under this condition exhibits high consistency.

Figure 8 shows the variations in the Kendall coefficient of different models under changes in the reinfection rate. KeyGAM-GCN performs best under all reinfection rate values, maintaining the highest Kendall coefficient, indicating that its key node identification ability is not affected by drastic changes in epidemic spreading parameters. At α=0.05, KeyGAM-GCN achieves 0.8453, demonstrating particularly stable key node identification performance under conditions of low reinfection probability.

6. Conclusions

This paper proposes KeyGAM-GCN model to identify the key nodes in the traportation networks, which integrate structure information and attribute information by leveraging adaptive feature learning to enhance model robustness under varying epidemic dynamics. KeyGAM-GCN outperforms seven baselines on ten networks, with a 37.24% average Kendall's tau improvement and about 4.20% gain in NDCG@K, while maintaining a low ISE. It remains robust and generalizes well across varying recovery and reinfection rates, surpassing traditional centrality and deep learning methods. In the future, the influence of real-world critical stations should be considered by incorporating richer operational data and historical event records.

Acknowledgment

This work is supported by the National Natural Science Foundation of China [No. 72101202] and Key Scientific and Technological Project of Henan Province [No. 252102221047].

References

1. Serdar M Z, Koç M, Al-Ghamdi S G. Urban transportation networks resilience: indicators, disturbances, and assessment methods. Sustainable Cities and Society 2022; 76: 103452. https://doi.org/10.1016/j.scs.2021.103452.
2. Pan X, Dang Y, Wang H, Hong D, Li Y, Deng H. Resilience model and recovery strategy of transportation network based on travel OD-grid analysis. Reliability Engineering & System Safety 2022; 223: 108483. https://doi.org/10.1016/j.ress.2022.108483.
3. Cheng J, Hu Z, Lu W, Wang K, Cai Z. A hybrid feature selection model for identifying groups of critical elements in aero-engine assembly. Quality and Reliability Engineering International 2024; 40(5): 2178–2195. https://doi.org/10.1002/qre.3515.
4. Saleem M, Abbas S, Ghazal T M, Khan M A, Sahawneh N, Ahmad M. Smart cities: Fusion-based intelligent traffic congestion control

system for vehicular networks using machine learning techniques. Egyptian Informatics Journal 2022; 23(3): 417–426. https://doi.org/10.1016/j.eij.2022.03.003.

5. Jin K, Wang W, Li X, Qin S. Exploring the robustness of public transportation system on augmented Network: A case from Nanjing China. Physica A: Statistical Mechanics and Its Applications 2022; 608(1): 128252. https://doi.org/10.1016/j.physa.2022.128252.
6. Dui H, Zhang Y, Chen L, Wu S. Cascading failures and maintenance optimization of urban transportation networks. Eksploatacja i Niezawodność-Maintenance and Reliability 2023; 25(3): 168826. https://doi.org/10.17531/ein/168826.
7. Veličković P. Everything is connected: Graph neural networks. Current Opinion in Structural Biology 2023; 79: 102538. https://doi.org/10.1016/j.sbi.2023.102538.
8. Szaciłło L, Jacyna M, Szczepański E, Izdebski M. Risk assessment for rail freight transport operations. Eksploatacja i Niezawodność-Maintenance and Reliability 2021; 23(3): 476–488. https://doi.org/10.17531/ein.2021.3.8.
9. Hua Z, Jing X, Martínez L. Consensus reaching for social network group decision making with ELICIT information: A perspective from the complex network. Information Sciences 2023; 627: 71–96. https://doi.org/10.1016/j.ins.2023.01.084.
10. Li R, Yuan X, Radfar M, Marendy P, Ni W, O'Brien T J. Graph signal processing, graph neural network and graph learning on biological data: a systematic review. IEEE Reviews in Biomedical Engineering 2021; 16: 109–135. https://doi.org/10.1109/RBME.2021.3122522.
11. Rozhkov A. Applying graph theory to find key leverage points in the transition toward urban renewable energy systems. Applied Energy 2024; 361: 122854. https://doi.org/10.1016/j.apenergy.2024.122854.
12. Meng B, Rezaeipanah A. Development of a multidimensional centrality metric for ranking nodes in complex networks.Chaos, Solitons and Fractals: the interdisciplinary journal of Nonlinear Science, and Nonequilibrium and Complex Phenomena 2025; 191: 115843. https://doi.org/10.1016/j.chaos.2024.115843.
13. Zhang Q, Deng R, Ding K, Li M. Structural analysis and the sum of nodes' betweenness centrality in complex networks. Chaos, Solitons & Fractals 2024; 185: 115158. https://doi.org/10.1016/j.chaos.2024.115158.
14. Evans T S, Chen B. Linking the network centrality measures closeness and degree. Communications physics 2022; 5(1): 172. https://doi.org/10.1038/s42005-022-00949-5.
15. Rafeeq B H, Pir R M, Sheikhahmadi A, Hamakarimi B R, Bahrani M. A method based on k-shell decomposition to identify influential nodes in complex networks. The Journal of Supercomputing 2023; 79(14): 15597–15622. https://doi.org/10.1007/s11227-023-05296-y.
16. Robert H F. A generalized eigenvector centrality for multilayer networks with inter-layer constraints on adjacent node importance. Applied Network Science 2024; 9: 14. https://doi.org/10.1007/s41109-024-00620-8.
17. Bihari A, Tripathi S, Deepak A. A review on h-index and its alternative indices. Journal of Information Science 2023; 49(3): 624–665. https://doi.org/10.1177/01655515211014478.
18. Noferini V, Wood R. Efficient computation of Katz centrality for very dense networks via negative parameter Katz. Journal of Complex Networks 2024; 12(5): cnae036. https://doi.org/10.1093/comnet/cnae036.
19. Liu Y, Liu J, Li Y. Automatic search of architecture and hyperparameters of graph convolutional networks for node classification. Applied Intelligence 2023; 53(9): 11104–11119. https://doi.org/10.1007/s10489-022-04096-w.
20. Huang K, Chen C. Subgraph generation applied in GraphSAGE deal with imbalanced node classification. Soft Computing 2024; 28(17): 10727–10740. https://doi.org/10.1007/s00500-024-09797-7.
21. Zhao G, Jia P, Zhou A, Zhang B. InfGCN: Identifying influential nodes in complex networks with graph convolutional networks. Neurocomputing 2020; 414: 18–26. https://doi.org/10.1016/j.neucom.2020.07.028.
22. Ali W, Vascon S, Stadelmann T, Pelillo M. Multi-view graph pooling via dominant sets for graph classification. Pattern Recognition 2025; 172(Part D): 112786. https://doi.org/10.1016/j.patcog.2025.112786.
23. Ye Z, Cai Z, Yang H, Si S, Zhou F. Joint optimization of maintenance and quality inspection for manufacturing networks based on deep reinforcement learning. Reliability engineering & system safety 2023; 236: 109290. https://doi.org/10.1016/j.ress.2023.109290.
24. Sun Z, Sun Y, Chang X, Wang F, Wang Q, Ullah A, Shao J. Finding critical nodes in a complex network from information diffusion and Matthew effect aggregation. Expert Systems with Applications 2023; 233: 120927. https://doi.org/10.1016/j.eswa.2023.120927.
25. Xu G, Dong C. CAGM: A communicability-based adaptive gravity model for influential nodes identification in complex networks. Expert Systems with Applications 2024; 235: 121154. https://doi.org/10.1016/j.eswa.2023.121154.

26. Lv L, Zhang T, Hu P, Bardou D, Niu S, Zheng Z, Yu G, Wu H. An improved gravity centrality for finding important nodes in multi-layer networks based on multi-PageRank. Expert Systems with Applications 2024; 238: 122171. https://doi.org/10.1016/j.eswa.2023.122171.
27. Wan C, Zhao Y, Zhang D, Yip T L. Identifying important ports in maritime container shipping networks along the Maritime Silk Road. Ocean & Coastal Management 2021; 211: 105738. https://doi.org/10.1016/j.ocecoaman.2021.105738.
28. Wen T, Gao Q, Chen Y, Cheong K H. Exploring the vulnerability of transportation networks by entropy: A case study of Asia–Europe maritime transportation network. Reliability Engineering & System Safety 2022; 226: 108578. https://doi.org/10.1016/j.ress.2022.108578.
29. Bai X, Ma Z, Zhou Y. Data-driven static and dynamic resilience assessment of the global liner shipping network. Transportation Research Part E: Logistics and Transportation Review 2023; 170: 103016. https://doi.org/10.1016/j.tre.2023.103016.
30. Xu M, Deng W, Zhu Y, Lu L. Assessing and improving the structural robustness of global liner shipping system: A motif-based network science approach. Reliability Engineering & System Safety 2023, 240: 109576. https://doi.org/10.1016/j.ress.2023.109576.
31. Dui H, Zheng X, Wu S. Resilience analysis of maritime transportation systems based on importance measures. Reliability Engineering & System Safety 2021; 209: 107461. https://doi.org/10.1016/j.ress.2021.107461.
32. He Z, Navneet K, van Dam W, van Mieghem P. Robustness assessment of multimodal freight transport networks. Reliability Engineering & System Safety 2021; 207: 107315. https://doi.org/10.1016/j.ress.2020.107315.
33. Du Z, Tang J, Qi Y, Wang Y, Han C, Yang Y. Identifying critical nodes in metro network considering topological potential: A case study in Shenzhen city—China. Physica A: Statistical Mechanics and its Applications 2020; 539: 122926. https://doi.org/10.1016/j.physa.2019.122926.
34. Sui Z, Wen Y, Huang Y, Zhou C, Du L, Piera M A. Node importance evaluation in marine traffic situation complex network for intelligent maritime supervision. Ocean Engineering 2022; 247: 110742. https://doi.org/10.1016/j.oceaneng.2022.110742.
35. Curado M, Tortosa L, Vicent J F. Identifying mobility patterns by means of centrality algorithms in multiplex networks. Applied Mathematics and Computation 2021; 406: 126269. https://doi.org/10.1016/j.amc.2021.126269.
36. Yang L, Wang J, Xie M. Graph-based reliability evaluation of a reconfigurable multi-stage system using sequential unconnected path sets. Reliability Engineering & System Safety 2025; 261: 111093. https://doi.org/10.1016/j.ress.2025.111093.
37. Zhang Y, Li L, Zhang W, Cheng Q. GATC and DeepCut: Deep spatiotemporal feature extraction and clustering for large-scale transportation network partition. Physica A: Statistical Mechanics and its Applications 2022; 606: 128110. https://doi.org/10.1016/j.physa.2022.128110.
38. Wandelt S, Shi X, Sun X. Estimation and improvement of transportation network robustness by exploiting communities. Reliability Engineering & System Safety 2021; 206: 107307. https://doi.org/10.1016/j.ress.2020.107307.
39. De Bona A A, de Oliveira Rosa M, Fonseca K V O, Luders R. A reduced model for complex network analysis of public transportation systems. Physica A: Statistical Mechanics and its Applications 2021; 567: 125715. https://doi.org/10.1016/j.physa.2020.125715.
40. Wei S, Zheng W, Wang L. Understanding the configuration of bus networks in urban China from the perspective of network types and administrative division effect. Transport Policy 2021; 104: 1–17. https://doi.org/10.1016/j.tranpol.2021.02.002.
41. Yang H, An S. Robustness evaluation for multi-subnet composited complex network of urban public transport. Alexandria Engineering Journal 2021; 60(2): 2065–2074, https://doi.org/10.1016/j.aej.2020.12.016.
42. Martín B, Ortega E, Cuevas-Wizner R, Ledda A, de Montis A. Assessing road network resilience: An accessibility comparative analysis. Transportation Research Part D: Transport and Environment 2021; 95: 102851. https://doi.org/10.1016/j.trd.2021.102851.
43. Izdebski M, Michalska A, Jacyna-Gołda I, Gherman L. Prediction of cyber-attacks in air transport using neural networks. Maintenance & Reliability/Eksploatacja i Niezawodność-Maintenance and Reliability 2024; 26(4):168826. https://doi.org/10.17531/ein/191476.
44. Huang X, Hu S, Wang W, Kaparias I, Zhong S, Na X. Identifying critical links in urban transportation networks based on spatio-temporal dependency learning. IEEE Transactions on Intelligent Transportation Systems 2023; 25(6): 5583–5597. https://doi.org/10.1109/TITS.2023.3339507.
45. Chen Y, Zhao P, Chen Q. Forecasting the commuting generation using metropolis-informed GCN and the topological commuter portrait. Transportation 2026; 53:483–510. https://doi.org/10.1007/s11116-024-10504-6.
46. Cui H, Chen S, Wang H, Meng Q. Network-level short-term traffic state prediction incorporating critical nodes: A knowledge-based deep fusion approach. Information Sciences 2024; 662: 120215. https://doi.org/10.1016/j.ins.2024.120215.

47. Liu Z, Qiu H, Guo W, Zhu J, Wang Q. NIE-GAT: node importance evaluation method for inter-domain routing network based on graph attention network. Journal of Computational Science 2022; 65: 101885. https://doi.org/10.1016/j.jocs.2022.101885.
48. Zhang M, Huang T, Guo Z, He Z. Complex-network-based traffic network analysis and dynamics: A comprehensive review. Physica A: Statistical Mechanics and its Applications 2022; 607: 128063. https://doi.org/10.1016/j.physa.2022.128063.
49. Zhao Y, Wang C, Rui Y, Lu W, Li L, Ran B. Bidirectional Temporal Convolutional Graph Attention Networks for Key Node Identification in Traffic Monitoring. IEEE Transactions on Intelligent Transportation Systems 2025; 26(6): 8720–8737. https://doi.org/10.1109/TITS.2025.3555540.
50. Silva D H, Rodrigues F A, Ferreira S C. Accuracy of discrete-and continuous-time mean-field theories for epidemic processes on complex networks. Physical Review E 2024; 110(1): 014302. https://doi.org/10.1103/PhysRevE.110.014302.
51. Essam F, El H, Ali S R H. A comparison of the pearson, spearman rank and kendall tau correlation coefficients using quantitative variables. Asian Journal of Probability and Statistics 2022; 20(3): 36–48. https://doi.org/10.9734/ajpas/2022/v20i3425.
52. Sun X, Sun F, Zhang Z, Li P, Wang S. Adaptive self-supervised learning for sequential recommendation. Neural Networks 2024; 179: 106570, https://doi.org/10.1016/j.neunet.2024.106570.
53. An B, Zhou X, Zhong Y, Yang T. SpatialRank: Urban Event Ranking with NDCG Optimization on Spatiotemporal Data. Advances in Neural Information Processing Systems 2023; 36: 9919–9930. https://doi.org/10.48550/arXiv.2310.00270.
54. Li Z, Zhang Q, Zhu F, Li D, Zheng C, Zhang F. Knowledge graph representation learning with simplifying hierarchical feature propagation. Information Processing & Management 2023; 60(4): 103348. https://doi.org/10.1016/j.ipm.2023.103348.
55. Yang H, Liu H, Zhang Y, Wu X. FMR-GNet: Forward Mix-Hop Spatial-Temporal Residual Graph Network for 3D Pose Estimation. Chinese Journal of Electronics 2024; 33(6): 1346–1359. https://doi.org/10.23919/cje.2022.00.365.
56. Pasa L, Navarin N, Erb W, Sperduti A. Empowering simple graph convolutional networks. IEEE Transactions on Neural Networks and Learning Systems 2023; 35(4): 4385-4399. https://doi.org/10.1109/TNNLS.2022.3232291.